1-1-2015

Aqueous preparation of surfactant-free copper selenide nanowires

Xinqi Chen
University of Wollongong, xc067@uowmail.edu.au

Zhen Li
University of Wollongong, zhenl@uow.edu.au

Jianping Yang
University of Wollongong, jpy546@uowmail.edu.au

Qiao Sun
University of Wollongong, qsun@uow.edu.au

S X. Dou
University of Wollongong, shi@uow.edu.au

Aqueous preparation of surfactant-free copper selenide nanowires

Abstract

Uniform surfactant-free copper selenide ($Cu_{2-x}Se$) nanowires were prepared via an aqueous route. The effects of reaction parameters such as Cu/Se precursor ratio, Se/NaOH ratio, and reaction time on the formation of nanowires were comprehensively investigated. The results show that $Cu_{2-x}Se$ nanowires were formed through the assembling of CuSe nanoplates, accompanied by their self-redox reactions. The resultant $Cu_{2-x}Se$ nanowires were explored as a potential thermoelectric candidate in comparison with commercial copper selenide powder. Both synthetic and commercial samples have a similar performance and their figures of merit are 0.29 and 0.38 at 750K, respectively.

Keywords

free, selenide, aqueous, nanowires, preparation, copper, surfactant

Disciplines

Engineering | Physical Sciences and Mathematics

Publication Details

Chen, X., Li, Z., Yang, J., Sun, Q. & Dou, S. (2015). Aqueous preparation of surfactant-free copper selenide nanowires. Journal of Colloid and Interface Science, 442 140-146.

Aqueous Preparation of Surfactant-free Copper Selenide Nanowires

Xinqi Chen,[a, c] *Zhen Li,*[a, b,]* *Jianping Yang,*[a] *Qiao Sun*[a,b] *and Shixue Dou*[a]

[a] Institute for Superconducting and Electronic Materials, Squires Way, Innovation Campus of University of Wollongong, Wollongong, NSW 2500, Australia.

[b] School of Radiation Medicine and Radiation Protection, Soochow University, 199 Ren Ai Road, Suzhou Industrial Park, Suzhou 215123, China.

[c] Institute of Nanoscience and Nanotechnology, Department of Physics, Central China Normal University, Wuhan, 430079, China.

[*]Corresponding author: zhenl@uow.edu.au; Tel: +61-2-42215163; Fax +61-2-42215731.

KEYWORDS: Semiconductor nanowires, copper selenide, surfactant free, aqueous preparation.

ABSTRACT Uniform surfactant-free copper selenide ($Cu_{2-x}Se$) nanowires were prepared via an aqueous route. The effects of reaction parameters such as Cu/Se precursor ratio, Se/NaOH ratio, and reaction time on the formation of nanowires were comprehensively investigated. The results show that $Cu_{2-x}Se$ nanowires were formed through the assembling of CuSe nanoplates, accompanied by their self-redox reactions. The resultant $Cu_{2-x}Se$ nanowires were explored as a potential thermoelectric candidate in comparison with commercial copper selenide powder. Both synthetic and commercial samples have a similar performance and their figures of merit are 0.29 and 0.38 at 750 K, respectively.

Introduction

Transition-metal chalcogenides have attracted considerable attentions due to their unique structures, novel properties and wide applications ranging from energy conversion/storage to biomedical field.[1-4] For example, both bulk and nano-scale copper selenides, despite their simple chemical formula, have very complicated crystal structures (e.g. tetragonal-, orthorhombic-, and cubic structures) and variable composition ($Cu_{2-x}Se$, $0 \leq x \leq 1$), which offer an incredible wealth of properties for diverse applications such as thermoelectric conversion, lithium-ion battery, photocatalysis, quantum-dot-sensitized solar cells, and photoacoustic imaging.[5-14] Nano-scale copper selenides exhibit some unusual properties due to the large surface area, high ratio of surface atoms, and quantum confinement effects. An example is the cuprous selenide (Cu_2Se) nanoparticles, which are easily oxidized into non-stoichiometric $Cu_{1.8}Se$, and become into surprisingly good *p*-type semiconductor with over 3000 times of enhancements in electrical conductivity.[2] In order to tune the properties of nano-scale copper selenides, a number of techniques and strategies, such as hydro- or solvo-thermal approach,[2, 15, 16] sonochemistry,[17] electrochemical-deposition,[18] microwave-assistant route,[19] ball milling technique,[6] and chemical welding method,[5] have been developed to prepare nanocrystals,[20] nanotubes/wires,[15, 21-23] nanocages,[24] dendrimers,[16, 25] and nanosheets[26] with well-defined size, morphology, crystal structure, and composition. However, most synthesises are complicated and the resultant nanostructures are stabilized with organic ligands, which could influence their properties (e.g. conductivity) and have to be removed in some applications. There are few reports on synthesis of surfactant-free copper selenide nanostructures, which can be used without post surface treatment.[27]

In comparison with zero dimensional (0D) and bulk counterparts, one dimensional (1D) semiconductor nanostructures have many unique characteristics including asymmetric structure, intrinsic polarization anisotropies, long (macroscopic) length, band and/or ballistic transport etc.[28-34] The electrons in nanowires are quantum confined laterally and thus occupy energy levels that are different from the traditional continuum of energy levels or bands found in bulk analogues. 1D semiconductor nanostructures show great potential in fabrication of various optical and electronic nanodevices.[35] For example, stoichiometric cuprous selenide nanowires have been utilized to fabricate catalytic electrode for oxygen reduction reaction,[36] and non-stoichiometric ones have been used to construct the photoluminescence type sensor of humidity.[37] In this work, we successfully synthesized uniform surfactant-free copper selenide ($Cu_{2-x}Se$) nanowire bundles on gram-scale via an aqueous route. The resultant $Cu_{2-x}Se$ nanowire bundles have diameters of 100-300 nm and lengths of tens of micrometers. The evolution of $Cu_{2-x}Se$ nanowires demonstrates they were formed through assembling of CuSe nanoplates accompanied by redox reaction. This gram-scale synthesis offers enough pristine nanowires for exploring their properties and potential applications. The nanowires were sintered into pellets for investigation of their thermoelectric properties, which show higher electrical conductivity, smaller Seebeck coefficient, and lower thermal conductivity than commercial Cu_2Se powder which was sintered and measured under the same conditions. The obtained *ZT* is comparable with that of commercial sample, and reach to 0.29 at 750 K.

Material and methods

Materials

Selenium powder (-325 mesh, 99.5%, Alfa Aesar), sodium hydroxide (low chloride, 97.0%, Alfa Aesar), copper nitrate 3-hydrate (99.5%, Aldrich), copper(I) selenide (99.95%, Alfa Aesar), copper powder (-40 mesh, 99.5%, Aldrich), and Milli-Q water (18.2 MΩ·cm) were used for the synthesis.

Synthesis of $Cu_{2-x}Se$ nanowires

In a typical synthesis, 0.158 g Se powder, 4.8 g NaOH (Se/NaOH = 1/60), and 20 mL Milli-Q water were loaded into a 100 mL round-bottomed flask. The mixture was heated to 90 ˚C under magnetic stirring. After the selenium was completely dissolved (deep red), 1.5 mL $Cu(NO_3)_2$ aqueous solution (0.5 M) [$Se/Cu(NO_3)_2$ = 2.5/1] was quickly added into the selenium solution. The black suspension was transferred into a 100 mL beaker, and then put into an oven at 100 ˚C until the water was completely evaporated. The black precipitate was washed with hot distilled water and centrifuged. The washing/centrifugation was repeated several times, and the purified sample was dried at 60 ˚C to constant weight. The yield is around 90%.

Crystal structure and morphology evolution of $Cu_{2-x}Se$ nanowires

In order to investigate the evolution of the morphology and crystal structure, a group of experiments was designed to prepare $Cu_{2-x}Se$ nanowires and collect the intermediate samples at different reaction times. The preparation procedure was the same as in the above process. Typically 1.5792 g Se powder, 48 g NaOH (Se/NaOH = 1/60), and 200 mL Milli-Q water were loaded into a 500 mL sealed round-bottomed flask. After the selenium was completely dissolved at 90 ˚C, the solution was equally divided into 10 beakers (20 mL in each beaker). After adding the same amount of 0.5 M $Cu(NO_3)_2$ aqueous solution (1.5 mL) [$Se/Cu(NO_3)_2$ = 2.5/1], all

beakers were kept in an oven at 100 ˚C, with the individual samples taken out at different times (i.e. 1 min, 40 min, 60 min, 90 min, 3.5 h, 5 h, 7 h, 9 h, 13 h, and 18 h).

In addition to normal oven, fan-forced oven and oil bath were also used to investigate the influence of heating manners on the evaporation of water. In this group of experiments, 0.316 g Se powder, 9.6 g NaOH, and 40 mL Milli-Q water were loaded into a 100 mL sealed round-bottomed flask. After the selenium was completely dissolved at 90 ˚C, the solution was equally divided and loaded into 2 beakers. After 1.5 mL $Cu(NO_3)_2$ aqueous solution (0.5 M) was quickly added into the selenium solution, the beakers were put into an oil bath in fume cupboard and a fan-forced oven separately at 100 ˚C until the water completely evaporated.

The influence of other reaction parameters on nanowires was also investigated. The procedures are similar and the resultant products were purified using the same process as described above.

Synthesis of $Cu_{2-x}Se$ from as-synthesized CuSe in alkaline solution

CuSe powder was synthesized by a solvent-mediated method, as described elsewhere.[38] 0.285 g CuSe powder was dispersed into 20 mL NaOH solution (0.12 M) (CuSe/NaOH = 1/60). The suspension was kept in an oven at 100 ˚C for 18 h. The resultant products were purified using the same process as described above.

Characterization

Powder X-ray diffraction (PXRD) patterns for all samples were collected using Cu $K\alpha_1$ radiation (λ = 1.5406 Å) at 40 kV and 25 mA with a position-sensitive detector. Energy dispersive X-ray spectroscopy (EDS), X-ray photoelectron spectroscopy (XPS), and inductively coupled plasma

atomic emission spectroscopy (ICP-AES) were used to characterize the chemical composition and crystal structure of the samples. The field emission scanning electron microscope (FE-SEM) images of all samples were collected using a JEOL JMS 7500-FA microscope with an accelerating voltage of 5 kV and a secondary electron detector. The transmission electron microscope (TEM) images were recorded on a JEOL 2011 microscope operated at 200 kV. The as-synthesized copper selenide nanowires were loaded into a graphite die with a diameter of 20 mm and sintered into a pellet at 703 K under 65 MPa for 10 min by the spark plasma sintering (SPS) technique. The resultant pellet was cut into pieces and polished into parallelepipeds with dimensions of ~2 mm × 3 mm × 10 mm. The parallelepipeds were coated with a layer of boron nitride to protect the instrument against evaporation of the elements. The electrical conductivity and the Seebeck coefficient were measured simultaneously under helium atmosphere from room temperature to 900 K using an Ozawa RZ2001i (Japan). A Linseis LFA1000 (Germany) instrument was used to determine the thermal diffusivity of samples that were cut and polished into a round shape with a diameter of 10 mm and a thickness of 1 mm. The thermal conductivity (κ) was calculated using Equation (1):

$$\kappa = D \times Cp \times \rho \quad (1)$$

where D is the thermal diffusivity, C_p is the heat capacity, and ρ is the mass density of the specimen. The ρ values used here were calculated using the geometrical dimensions of the specimens and their masses. The heat capacity was determined using the differential scanning calorimetry (DSC) method.

Results and discussion

Copper selenide nanowires were prepared from copper nitrate and selenium in sodium hydroxide solution. Figure 1 shows the X-ray diffraction (XRD) pattern, and scanning and transmission electron microscope (SEM and TEM) images of the resultant nanowires. Compared with the standard diffraction peaks of copper selenide, all the peaks of our nanowires match well with those of face-centred-cubic $Cu_{2-x}Se$ (JCPDS 06-0680) with a lattice constant of 0.5728 nm [Figure 1(a)]. The strong and sharp diffraction peaks suggest that the as-synthesized nanowires are well crystallized. The absence of other peaks indicates high purity and the single-phase nature of these nanowires. The typical field emission SEM (FESEM) image in Figure 1(b) clearly shows a large quantity of uniform bundles with lengths up to tens of micrometers and diameters of 100-300 nm. A typical bundle is displayed in Figure 1(b) as an inset. A high-resolution SEM image reveals that each bundle is assembled from many thin nanowires (Figure S1 in the Supporting Information). The TEM image in Figure 1(c) also confirms that these bundles have a uniform diameter and that they are made up of many thin nanowires. The high-resolution TEM (HRTEM) image clearly shows the lattice fringes with a spacing of 0.33 nm [Figure 1(d)], which matches well with that of (111) planes of $Cu_{2-x}Se$. Both XRD and HRTEM prove that the resultant nanowires are non-stoichiometric $Cu_{2-x}Se$ rather than stoichiometric Cu_2Se. The energy-dispersive X-ray spectrum (EDS) in Figure S2 shows that the ratio of copper to selenium in these nanowire bundles is 1.84, which is higher than the initial precursor ratio (Cu/Se = 1/2.5) and further confirms that they are Cu-deficient.

In order to understand the formation mechanism of the $Cu_{2-x}Se$ nanowires, we repeated the experiment and collected the intermediate products at different reaction times. Figure 2 shows the XRD patterns of the samples collected at 1 min, 40 min, 3.5 h, 5 h, and 18 h. When the copper nitrate solution reacted with Se-precursor solution for 1 min, the XRD pattern of the

product [Figure 2(a)] matched that of hexagonal CuSe (JCPDS 34-0171). After 40 minutes reaction, the XRD pattern of the products is still indexed to hexagonal CuSe [Figure 2(b)]. When the mixture reacted for 3.5 h, the intermediate product is a mixture of hexagonal CuSe and cubic $Cu_{2-x}Se$ [Figure 2(c)]. The diffraction peaks marked with * arise from $Cu_{2-x}Se$ (JCPDS 06-0680). The intermediate product collected at 5 h is also a mixture of CuSe and $Cu_{2-x}Se$ [Figure 2(d)], but the content of CuSe is notably decreased due to the formation of $Cu_{2-x}Se$. The final product collected at 18 h shows single phase $Cu_{2-x}Se$ [Figure 2(e)], which demonstrates the complete transformation of CuSe into $Cu_{2-x}Se$. The transformation of CuSe into $Cu_{2-x}Se$ is also supported by the variation of the Cu/Se molar ratio in these samples, as determined by inductively coupled plasma atomic electron spectroscopy (ICP-AES) and shown in Table 1. The results clearly show the increase in the Cu/Se molar ratio during the transformation process. When the $Cu(NO_3)_2$ solution was added into the alkaline selenium solution, the black precipitate formed immediately and its Cu/Se molar ratio was 1.01, which means the main product is CuSe. When the reaction time increased from 1 min, through 40 min, 90 min, 3.5 h, 5 h, and 7 h, to 18 h, the Cu/Se molar ratio in these samples correspondingly increased from 1.01, through 1.06, 1.35, 1.51, 1.51, and 1.52, to 1.65.

The above results support the formation of non-stoichiometric $Cu_{2-x}Se$ nanowires, and the reduction of Cu^{2+} into Cu^{+} during sample preparation. X-ray photoelectron spectroscopy (XPS) was used to determine the ratio of Cu^{2+}/Cu^{+} in these samples, and the whole XPS survey and spectra of Cu $2p_{3/2}$ are presented in Figure 3 (a-c). A slight shift in the binding energy of Cu $2p_{3/2}$ from 932.07 eV to 931.52 eV was observed when the reaction time increased from 1 min to 18 h [Figure 3(b)]. The small shift indicates the difficulty in distinguishing the contributions from Cu^{2+} and Cu^{+}. The binding energy of Cu $2p_{3/2}$ can be fitted into three peaks at 931.98 eV (CuSe),

931.48 eV (Cu_2Se), and 933.87 eV (CuO) [Figure 3(c)]. At the very beginning of the reaction, there are only Cu^{2+} peaks. The Cu^{2+}/Cu^{+} ratio from CuSe and Cu_2Se in the samples collected at 40 min and 7 h decreased from 3.88 to 0.33 [Figure S3(b-g)], which means that the reduction of Cu^{2+} into Cu^{+} occurred upon the addition of copper nitrate solution to the Se-precursor solution. The absence of a contribution from CuSe in the sample collected at 18 h supports the complete transformation of CuSe into $Cu_{2-x}Se$. The small peak at 933.87 eV (CuO) in all samples is attributed to surface oxidation.[2, 39, 40]

The evolution of the morphology during the transformation was monitored by SEM. Figure 4 shows SEM images of eight samples collected at different reaction times, 1 min, 40 min, 60 min, 90 min, 3.5 h, 5 h, 7 h, and 18 h, respectively. At the first stage (i.e. from 1 min to 60 min), the initially formed CuSe nanoparticles grow into hexagonal nanoplates with a size of 100-400 nm, as shown in Figure 4(a-c). At the second stage (i.e. from 60 min to 5 h), the hexagonal nanoplates become stacked together and self-assemble into a one-dimensional structure with a rough surface [Figure 4(d-f)]. The products are a mixture of CuSe and $Cu_{2-x}Se$, as proved by their XRD patterns in Figure 2. At the last stage (i.e. from 5 h to 18 h), the rough nanowire bundles become smoother [Figure 2(g-h)], which is accompanied by the complete transformation of CuSe into $Cu_{2-x}Se$ (Figure 2). The final nanowire bundles are about 100-300 nm in diameter and tens of micrometers in length.

The evaporation rate of solvent significantly influenced the assembling of nanoplates. We used oil bath and fan-forced oven to replace normal oven to induce water evaporation at the same temperature. It only took 7 h and 11 h for water evaporating completely, shorter than use of normal oven. As shown in Figure S4(a-b), the surface of nanowire bundles are rough, and stuck with some nanoplates, which means the nanoplates can’t assemble into uniform nanowires due to

the faster evaporation of water. Other reaction parameters such as precursor concentration also influenced the final nanowire bundles. For example, thinner $Cu_{2-x}Se$ nanowire bundles (~100 nm) shown in Figure S4(c) can be prepared by decreasing Se powder (from 0.158 g to 0.079 g) and $Cu(NO_3)_2$ aqueous solution (from 1.5 mL to 0.75 mL).

It should be noted that the morphology and composition of the nanowires are strongly influenced by the reaction parameters. Figure S6 shows the XRD patterns of products prepared using different molar ratios of sodium hydroxide to selenium powder (i.e. NaOH/Se). When a high molar ratio of NaOH/Se (i.e. 60/1) is used [Figure S6(a)], the final product is pure $Cu_{2-x}Se$, and its XRD pattern is consistent with the standard profile of $Cu_{2-x}Se$ indexed with JCPDS 06-0680. When the molar ratio is decreased from 60/1 to 30/1, the product obtained is a mixture of $Cu_{2-x}Se$, Cu_2O, and CuO. The diffraction peaks of Cu_2O and CuO are marked with $^{\#}$ and ^{o}, respectively in Figure S6(b). Their SEM images in Figure S7 show that the sample prepared with a high NaOH/Se ratio has uniform nanowire bundles [Figure S7(a)], while the sample obtained with a low NaOH/Se ratio contains some big plates and particles in addition to the nanowire bundles [Figure S7(b)]. This result demonstrates the importance of the NaOH/Se ratio for the formation of uniform nanowires.

In addition, the molar ratio of the selenium powder to the copper nitrate also strongly affects the product morphology and composition. Figure S8 shows the XRD patterns of products prepared by adding different amounts of copper nitrate to the same amount of alkaline selenium aqueous solution, i.e. the Se/Cu ratio is varied from 0.5/1, though 1/1, 2.5/1, and 5/1, to 10/1. In the case of the lowest Se/Cu precursor ratio (i.e. 0.5/1), the small amount of selenium is not enough for a complete reaction with copper nitrate, and the excess copper nitrate is hydrolysed and dehydrated to form Cu_2O, whose diffraction peaks are labelled with $^{\Delta}$ in Figure S8(a). In the

opposite case (i.e. Se/Cu ratio of 10/1), the large amount of selenium leads to the formation of CuSe [marked with ♦ in Figure S8(e)] mixed with $Cu_{2-x}Se$. When the precursor molar ratio is in the range of 1/1 to 5/1, the final products obtained are pure $Cu_{2-x}Se$, as confirmed by their XRD patterns shown in Figure S8(b-d). Their SEM images in Figure S9 demonstrate that uniform nanowires can be only obtained from a molar ratio of 2.5/1. Therefore, the optimal molar ratio of selenium powder to copper nitrate is 2.5/1.

On the basis of previous results, we proposed the following mechanism. After the copper nitrate solution is added into the selenium precursor solution, the competition among reactions (2)–(4) is strongly dependent on the solubility constants of CuSe ($K_{sp} = 7.94 \times 10^{-49}$), $CuSeO_3$ ($K_{sp} = 2.1 \times 10^{-8}$), and Cu_2Se ($K_{sp} = 1.58 \times 10^{-61}$).[23] For the same Se^{2-} concentration, the minimum Cu^{2+} concentration required for precipitation of CuSe is smaller than that required for Cu_2Se and $CuSeO_3$. Thus, CuSe was first precipitated after the addition of copper nitrate solution to selenium solution. The formation Gibbs free energy (ΔG) can be expressed by Equation (5), in which R is the universal gas constant, T is the temperature, K_{sp} is the solubility of CuSe. J_{sp} is expressed by Equation (6), where $C_{Cu}{}^{2+}$ and $C_{Se}{}^{2-}$ represent the concentration of Cu^{2+} and Se^{2-}, respectively.

$$3Se + 6NaOH \rightarrow 2Na_2Se + Na_2SeO_3 + 3H_2O \quad (1)$$

$$Cu(NO_3)_2 + Na_2Se \rightarrow CuSe + 2NaNO_3 \quad (2)$$

$$Cu(NO_3)_2 + Na_2SeO_3 \rightarrow CuSeO_3 + 2NaNO_3 \quad (3)$$

$$2Cu(NO_3)_2 + 2Na_2Se \rightarrow Cu_2Se + Se + 4NaNO_3 \quad (4)$$

$$\Delta G = RT \times \ln J_{sp}/K_{sp} \quad (5)$$

$$J_{sp} = C_{Cu^{2+}}^2 \times C_{Se^{2-}}^2 \quad (6)$$

$$(2-x)CuSe \rightarrow Cu_{2-x}Se + (1-x)Se \quad (7)$$

The high concentrations of Cu^{2+} and Se^{2-}, and small K_{sp} (7.94×10^{-49}) of CuSe indicate a large ΔG for the formation of CuSe nanoparticles. In addition, from viewpoint of nucleation and growth of nanocrystals, high precursor concentration means the fast nucleation and growth process, which leads to a broad particle size distribution. Therefore, a mixture of nanoparticles and nanoplates is obtained upon the addition of copper nitrate solution into selenium precursor solution. The nanoparticles can be transformed into nanoplates through the Oswald ripening process due to the intrinsic layered structure.

The transformation of nanoplates into nanowires is induced by water evaporation, which increases the concentration of nanoplates and promotes their self-assembly in longitudinal direction (i.e. [110] direction). During the evaporation process, solvent flow caused by H2O evaporation helps to transfer CuSe nanoplates for their longitudinally self-assembly. Meanwhile, the long-range interactive force, induced by the surface tension of the solvent and the attractive interaction between the nanoplates may contribute to the stacking of CuSe plates as well as the self-assembly of the CuSe nanoplates into $Cu_{2-x}Se$ bundle structures. The transformation of CuSe into $Cu_{2-x}Se$ by the self oxidation-reduction reaction can be easily achieved in strong NaOH solution [formula (7)], which has been proved by treating CuSe powder in the same NaOH solution without other chemicals (Figure S10).

As mentioned previously, $Cu_{2-x}Se$ nanostructures show high electrical conductivity arising from pronounced Cu deficiency. Bulk $Cu_{2-x}Se$ and Cu_2Se have potential in thermoelectric application due to the liquid-like behaviour of Cu^+ ions at high temperature. We therefore compare the thermoelectric properties of our $Cu_{2-x}Se$ nanowires with commercial Cu_2Se powders. The reason we selected Cu_2Se is that there is no commercial $Cu_{2-x}Se$ powder and it is

very difficult to prepare stoichiometric Cu_2Se nanowires using our approach. Nevertheless, the comparison between them would demonstrate the nano effects on their thermoelectric properties.

Both synthetic and commercial powders were sintered under the same conditions (i.e. 703 K, 65 MPa, 10 min) using the spark plasma sintering (SPS) technique. The resultant pellets were cut into pieces with a similar size and then measured under the same conditions (Figure 5). The electrical conductivity [Figure 5(a)] of the $Cu_{2-x}Se$ sample is around 6800 S/cm at room temperature and decreases quickly to about 2200 S/cm at 750 K, which is higher than that of commercial Cu_2Se powder at room temperature (2600 S/cm) and at 750 K (1200 S/cm), respectively. The higher electrical conductivity of $Cu_{2-x}Se$ is due to its higher Cu-deficiency compared to commercial Cu_2Se, which is consistent with previous report.[41] Due to its excellent electrical conductivity, the Seebeck coefficient [Figure. 5(b)] of $Cu_{2-x}Se$ is lower than that of commercial Cu_2Se (i.e. 35 μV/K at room temperature and 80 μV/K at 750 K). Having the same trend as the Seebeck coefficient, this sample has a power factor [Figure 5(c)] of 0.3 $\mu Wcm^{-1}K^{-2}$ at room temperature and 5 $\mu Wcm^{-1}K^{-2}$ at 750 K, lower than that of commercial sample.

To determine the thermal conductivity of samples, their heat capacities (*Cp*) were measured and shown in Figure 5(d). A sharp endothermal peak at around 400 K was observed in both synthetic and commercial samples, which is consistent with the previous reports (e.g. blue line in Figure S11).[6] The overall thermal conductivity can be calculated by using Equation (1). The resultant total thermal conductivity [Figure 5(e)] of our $Cu_{2-x}Se$ sample from room temperature to 470 K is higher than that of the commercial Cu_2Se sample, however it is slightly lower in the range of 470 – 750 K. The lower total thermal conductivity of synthetic $Cu_{2-x}Se$ could be due to the presence of nanoprecipitates in the pellet, which can effectively improve the phonon scattering and decrease the thermal conductivity. The SEM images of pellets made from $Cu_{2-x}Se$

nanowires and commercial Cu_2Se powder in Figure S12 clearly show that the $Cu_{2-x}Se$ nanowires were melted into nanoprecipitates at high temperature (703 K) and high pressure (65 MPa) after SPS sintering, while the commercial Cu_2Se powder was pressed into a bulk layer structure. In addition, the pronounced Cu-deficiency in the synthetic sample leads to more vacancies, which are also responsible for its lower thermal conductivity. The figure of merit for synthetic and commercial samples can be calculated by Equation (2).

$$ZT = \frac{S^2 \sigma T}{k} \quad (2)$$

where S, σ, κ, and T are the Seebeck coefficient, the electrical conductivity, the thermal conductivity, and the absolute temperature, respectively.[42-44] The calculated ZT values of $Cu_{2-x}Se$ and Cu_2Se samples were plotted in Figure 5(f), a slight decrease in ZT at 400 K was observed due to the presence of sharp endothermal peak at this temperature [Figure 5(d)]. The ZT values of synthetic and commercial samples increase with the increase of temperature, and reach 0.29 and 0.38 at 750 K, respectively. Our results are similar to that of $Cu_{2-x}Se$ ($0 \leq x \leq 0.25$) prepared from a high-temperature solid state reaction, in which the highest ZT is from Cu_2Se with a value of 0.38 at 750 K.[5, 41]

Conclusions

In summary, surfactant-free $Cu_{2-x}Se$ nanowire bundles with lengths of tens of micrometers and diameters of 100–300 nm have been successfully synthesized on a large scale by an aqueous approach. The nanowire bundles are composed of many thin $Cu_{2-x}Se$ nanowires. The evolution of the morphology shows that the formation of $Cu_{2-x}Se$ nanobundles arises from the assembly of CuSe nanoplates induced by water evaporation, accompanied by the self oxidation-reduction of CuSe. The formation of $Cu_{2-x}Se$ nanobundles is strongly influenced by the molar ratio of sodium

hydroxide to selenium powder, and the molar ratio of selenium powder to copper nitrate. The resultant $Cu_{2-x}Se$ nanobundles were sintered into pellet and tested for thermoelectric application in comparison with commercial Cu_2Se powder. The results show that the synthetic sample has a temperature-dependent *ZT* comparable to that of commercial sample, and reach to 0.29 at 750 K. Our research provides a straight way to prepare surfactant-free copper selenide nanowires for energy conversion.

Acknowledgments

X. Chen gratefully acknowledges the Chinese Scholarship Council (CSC) (201206770014) and Central China Normal University (2011011218) for her scholarship. Z. Li acknowledges support from the Australian Research Council (ARC) through the Discovery Project DP130102699 and DP130102274. S. Dou is grateful for support from the Baosteel-Australia Research Centre (BARC) through the project BA110011 and to the ARC through the Linkage Project LP120200289. The authors also appreciate support from the Electron Microscopy Centre at UOW, and thank Dr. Tania Silver for critical reading of the manuscript, and also thank Prof. Ren's group for kindly providing heat capacity data.

References

[1] Y.X. Zhao, C. Burda, Energy Environ. Sci. 5 (2012) 5564.
[2] S.C. Riha, D.C. Johnson, A.L. Prieto, J. Am. Chem. Soc. 133 (2011) 1383.
[3] I. Kriegel, C.Y. Jiang, J. Rodriguez, R.D. Schaller, D.V. Talapin, E. Como, J. Feldmann, J. Am. Chem. Soc. 134 (2012) 1583.
[4] I. Kriegel, J. Rodriguez, A. Wisnet, H. Zhang, C. Waurisch, A. Eychmuller, A. Dubavik, A.O. Govorov, J. Feldmann, ACS Nano 7 (2013) 4367.
[5] H.L. Liu, X. Shi, F.F. Xu, L.L. Zhang, W.Q. Zhang, L.D. Chen, Q. Li, C. Uher, T. Day, G.J. Snyder, Nat. Mater. 11 (2012) 422.

[6] B. Yu, W.S. Liu, S. Chen, H. Wang, H.Z. Wang, G. Chen, Z.F. Ren, Nano Energy 1 (2012) 472.
[7] C. Han, Z. Li, S.X. Dou, Chin. Sci. Bull. 59 (2014) 2073.
[8] C.H. Lai, K.W. Huang, J.H. Cheng, C.Y. Lee, B.J. Hwang, L.J. Chen, J. Mater. Chem. 20 (2010) 6638.
[9] J.L. Yue, Q. Sun, Z.W. Fu, Chem. Commun. 49 (2013) 5868.
[10] C. Han, Z. Li, W.J. Li, S.L. Chou, S.X. Dou, J. Mater. Chem. A 2 (2014) 11683.
[11] Y. Liu, Y. Deng, Z. Sun, J. Wei, G. Zheng, A.M. Asiri, S.B. Khan, M.M. Rahman, D. Zhao, Small 9 (2013) 2702.
[12] Z.S. Yang, C.Y. Chen, C.W. Liu, C.L. Li, H.T. Chang, Adv. Energy Mater. 1 (2011) 259.
[13] J.N. Anker, W.P. Hall, O. Lyandres, N.C. Shah, J. Zhao, R.P. Van Duyne, Nat. Mater. 7 (2008) 442.
[14] X.Q. Chen, Z. Li, Y. Bai, Q. Sun, L.Z. Wang, S.X. Dou, Chem. Eur. J. (2014), DOI 10.1002/chem. 201405354.
[15] Y. Zhang, C.G. Hu, C.H. Zheng, Y. Xi, B.Y. Wan, J. Phys. Chem. C 114 (2010) 14849.
[16] D.P. Li, Z. Zheng, Y. Lei, S.X. Ge, Y.D. Zhang, Y.G. Zhang, K.W. Wong, F.L. Yang, W.M. Lau, CrystEngComm 12 (2010) 1856.
[17] Y.X. Zhao, H.C. Pan, Y.B. Lou, X.F. Qiu, J.J. Zhu, C. Burda, J. Am. Chem. Soc. 131 (2009) 4253.
[18] R. Yu, T. Ren, K.J. Sun, Z.C. Feng, G.N. Li, C. Li, J. Phys. Chem. C 113 (2009) 10833.
[19] X.B. Cao, C. Zhao, X.M. Lan, G.J. Gao, W.H. Qian, Y. Guo, J. Phys. Chem. C 111 (2007) 6658.
[20] S. Deka, A. Genovese, Y. Zhang, K. Miszta, G. Bertoni, R. Krahne, C. Giannini, L. Manna, J. Am. Chem. Soc. 132 (2010) 8912.
[21] J. Xu, W.X. Zhang, Z.H. Yang, S.H. Yang, Inorg. Chem. 47 (2008) 699.
[22] Y. Jiang, Y. Wu, B. Xie, S.Y. Zhang, Y.T. Qian, Nanotechnology 15 (2004) 283.
[23] J. Xu, W.X. Zhang, Z.H. Yang, S.X. Ding, C.Y. Zeng, L.L. Chen, Q. Wang, S.H. Yang, Adv. Funct. Mater. 19 (2009) 1759.
[24] H.L. Cao, X.F. Qian, J.T. Zai, J. Yin, Z.K. Zhu, Chem. Commun. (2006) 4548.
[25] J.B. Zhu, Q.Y. Li, L.F. Bai, Y.F. Sun, M. Zhou, Y. Xie, Chem. Eur. J. 18 (2012) 13213.
[26] Y. Xie, X.W. Zheng, X.C. Jiang, J. Lu, L.Y. Zhu, Inorg. Chem. 41 (2002) 387.
[27] W.X. Zhang, X.M. Zhang, L. Zhang, J.X. Wu, Z.H. Hui, Y.W. Cheng, J.W. Liu, Y. Xie, Y.T. Qian, Inorg. Chem. 39 (2000) 1838.
[28] Z. Li, L.N. Cheng, Q. Sun, Z.H. Zhu, M.J. Riley, M. Aljada, Z.X. Cheng, X.L. Wang, G.R. Hanson, S.Z. Qiao, S.C. Smith, G.Q. Lu, Angew. Chem. Int. Edit. 49 (2010) 2777.
[29] Z. Li, O. Kurtulus, N. Fu, Z. Wang, A. Kornowski, U. Pietsch, A. Mews, Adv. Funct. Mater. 19 (2009) 3650.
[30] A. Myalitsin, C. Strelow, Z. Wang, Z. Li, T. Kipp, A. Mews, ACS Nano 5 (2011) 7920.
[31] Z. Li, Q. Sun, Z.H. Zhu, S.C. Smith, G.Q. Lu, One-dimensional nanostructures: Principles and applications, ed. T.Y. Zhai and J.N. Yao, Wiley (2013).
[32] Z. Li, A.J. Du, Q. Sun, M. Aljada, L.N. Cheng, M.J. Riley, Z.H. Zhu, Z.X. Cheng, X.L. Wang, J. Hall, E. Krausz, S.Z. Qiao, S.C. Smith, G.Q.M. Lu, Chem. Commun. 47 (2011) 11894.
[33] Z. Li, X.D. Ma, Q.A. Sun, Z. Wang, J.A. Liu, Z.H. Zhu, S.Z. Qiao, S.C. Smith, G.Q. Lu, A. Mews, Eur. J. Inorg. Chem. (2010) 4325.
[34] M. Tan, X.Q. Chen, J. Electrochem. Soc. 159 (2012) K15.
[35] Z. Li, A.J. Du, Q. Sun, M. Aljada, Z.H. Zhu, G.Q. Lu, Nanoscale 4 (2012) 1263.

[36] S.L. Liu, Z.S. Zhang, J.C. Bao, Y.Q. Lan, W.W. Tu, M. Han, Z.H. Dai, J. Phys. Chem. C 117 (2013) 15164.
[37] A. Jagminas, R. Juskenas, I. Gailiute, G. Statkute, R. Tomasiunas, J. Cryst. Growth 294 (2006) 343.
[38] P. Kumar, M. Gusain, R. Nagarajan, Inorg. Chem. 51 (2012) 7945.
[39] M. Sykora, A.Y. Koposov, J.A. McGuire, R.K. Schulze, O. Tretiak, J.M. Pietryga, V.I. Klimov, ACS Nano 4 (2010) 2021.
[40] N.S. Mcintyre, M.G. Cook, Anal. Chem. 47 (1975) 2208.
[41] X.X. Xiao, W.J. Xie, X.F. Tang, Q.J. Zhang, Chin. Phys. B 20 (2011) 087201.
[42] B. Poudel, Q. Hao, Y. Ma, Y.C. Lan, A. Minnich, B. Yu, X.A. Yan, D.Z. Wang, A. Muto, D. Vashaee, X.Y. Chen, J.M. Liu, M.S. Dresselhaus, G. Chen, Z.F. Ren, Science 320 (2008) 634.
[43] Y. Ma, Q. Hao, B. Poudel, Y.C. Lan, B. Yu, D.Z. Wang, G. Chen, Z.F. Ren, Nano Lett. 8 (2008) 2580.
[44] G. Joshi, H. Lee, Y.C. Lan, X.W. Wang, G.H. Zhu, D.Z. Wang, R.W. Gould, D.C. Cuff, M.Y. Tang, M.S. Dresselhaus, G. Chen, Z.F. Ren, Nano Lett. 8 (2008) 4670.

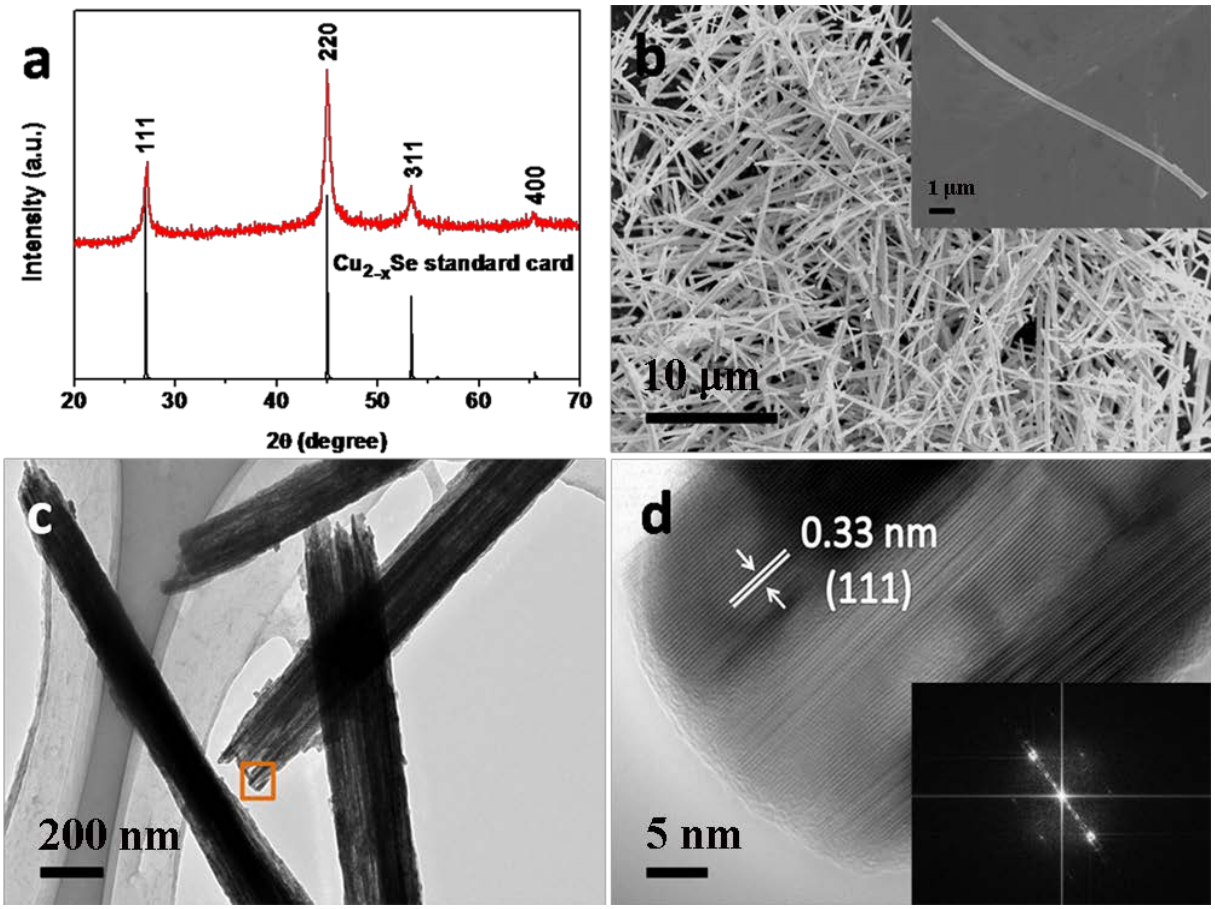

Figure 1. (a) XRD pattern of surfactant-free $Cu_{2-x}Se$ nanowire bundles prepared from copper nitrate and selenium NaOH solution. The vertical lines mark the line positions of the $Cu_{2-x}Se$ standard (JCPDS 06-0680). (b) Field emission SEM (FESEM) images of the resultant $Cu_{2-x}Se$ nanowire bundles. Inset is a typical image of an individual bundle. (c) TEM image of the $Cu_{2-x}Se$ nanowire bundles, showing that each bundle is composed of many thin nanowires. (d) HRTEM image of the selected area in Figure 1c. Insets are fast fourier transform (FFT) of HRTEM image of the selected area in c.

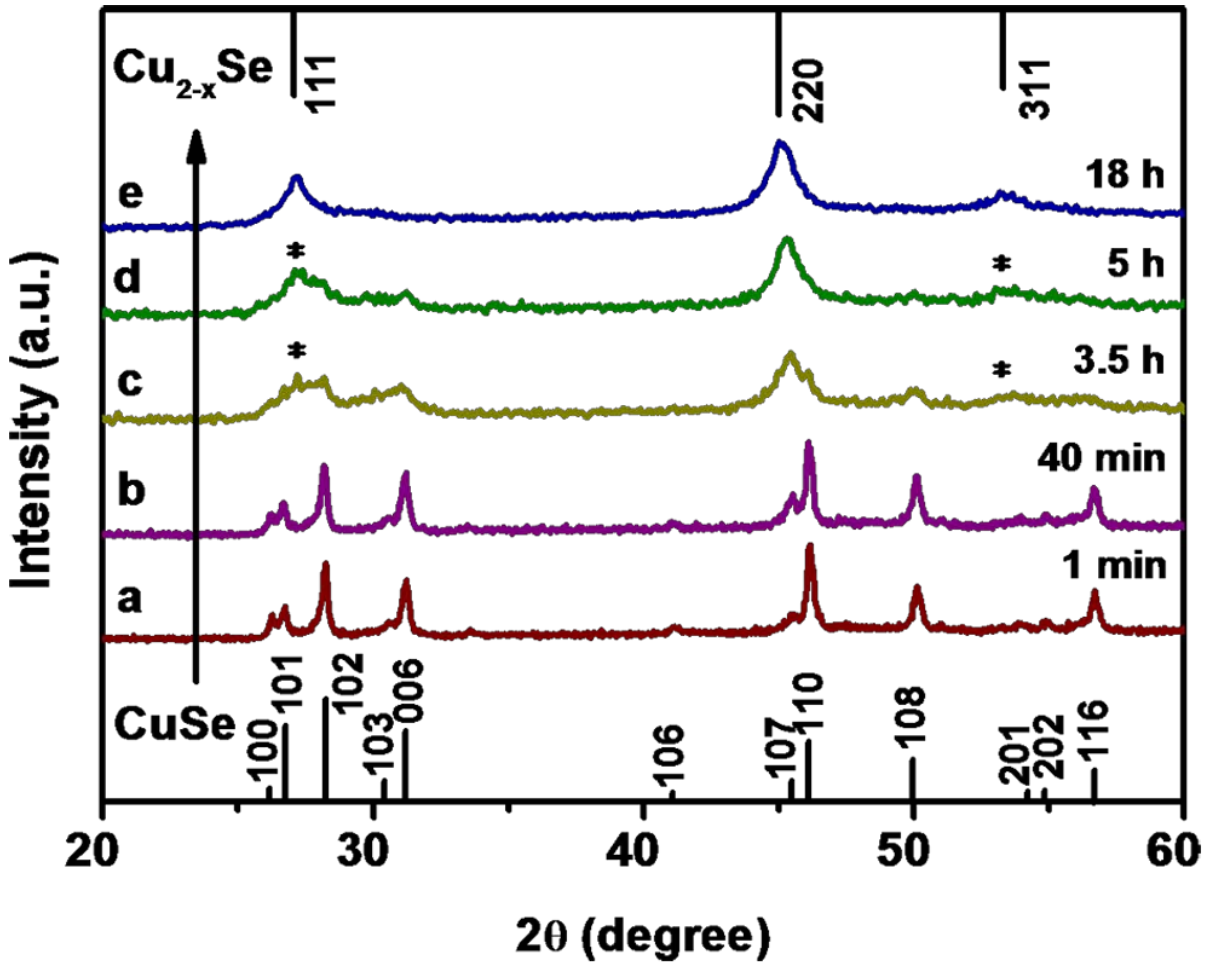

Figure 2. XRD patterns of copper selenide samples collected at (a) 1 min, (b) 40 min, (c) 3.5 h, (d) 5 h, and (e) 18 h, showing the transformation of the crystal structure from hexagonal CuSe into cubic $Cu_{2-x}Se$. The diffraction peaks marked with * arise from $Cu_{2-x}Se$ (JCPDS 06-0680).

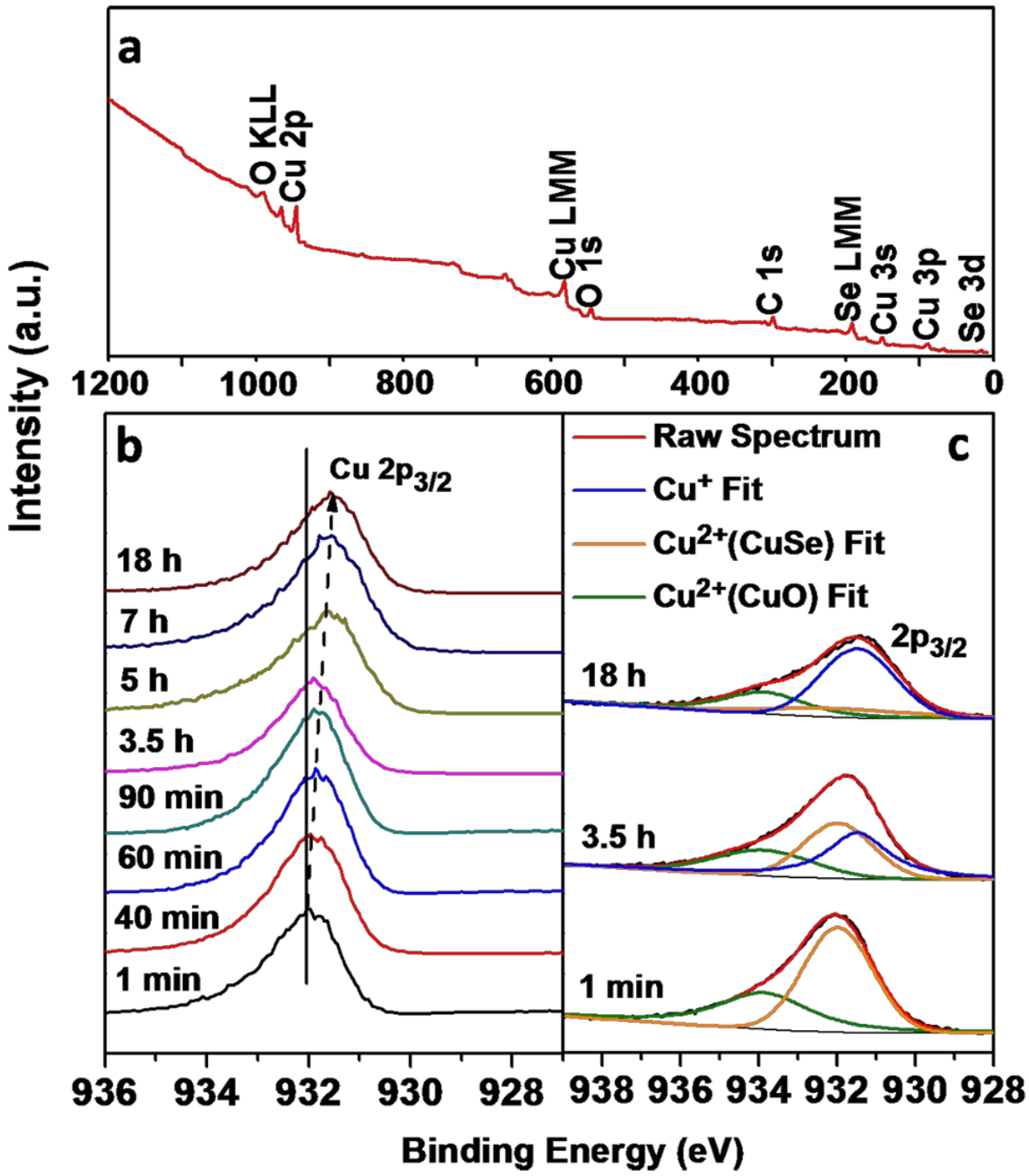

Figure 3. (a) Whole survey of as prepared $Cu_{2-x}Se$ nanowires; (b) Binding energies of Cu $2p_{3/2}$ in the products collected from 1 min to 18 h; (c) XPS spectra of the Cu $2p_{3/2}$ region for selected samples with peak fits for Cu^{2+} and Cu^{+}.

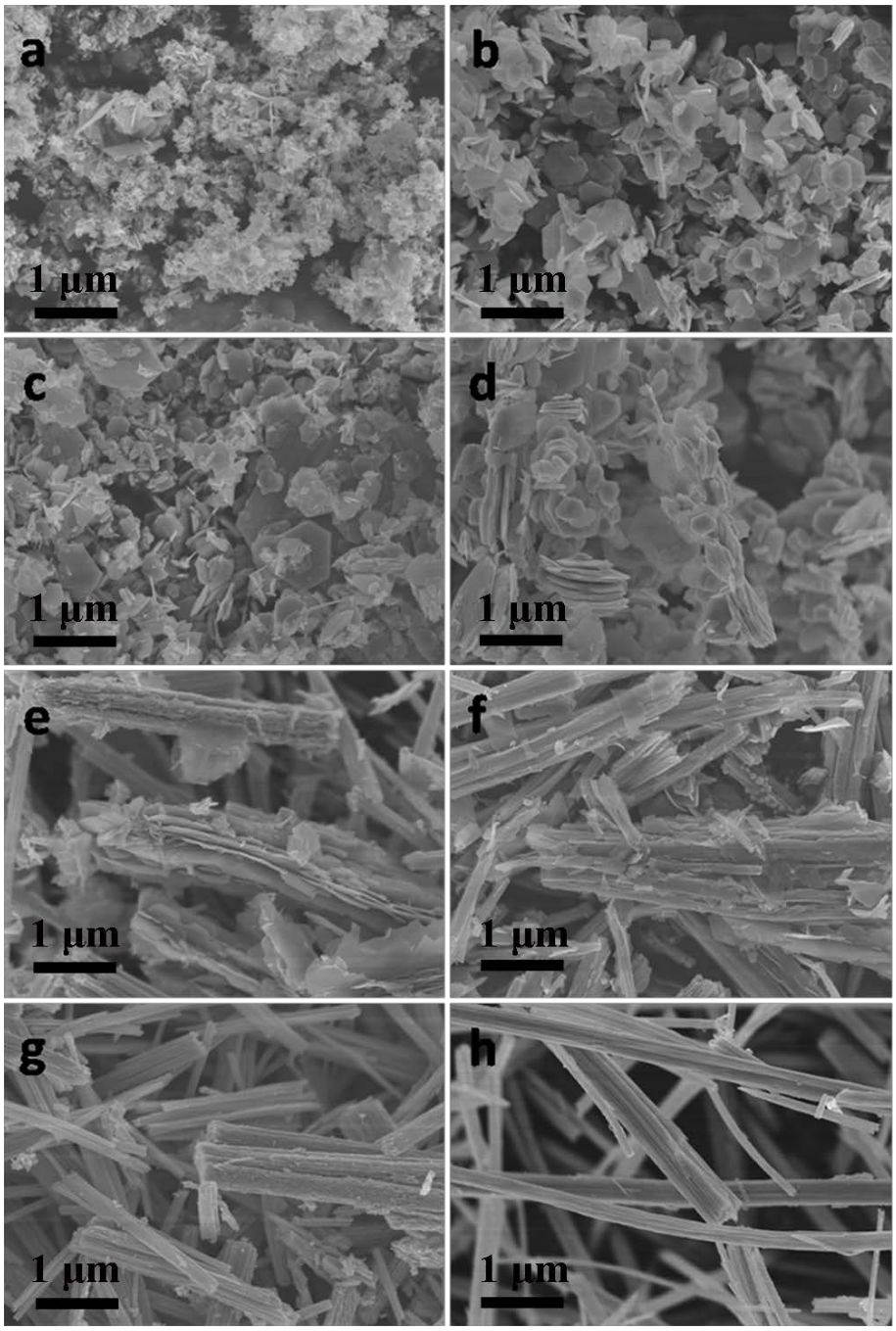

Figure 4. FESEM images of the copper selenides collected at (a) 1 min, (b) 40 min, (c) 60 min, (d) 90 min, (e) 3.5 h, (f) 5 h, (g) 7 h, and (h) 18 h, showing the evolution of the morphology of the $Cu_{2-x}Se$ nanowire bundles.

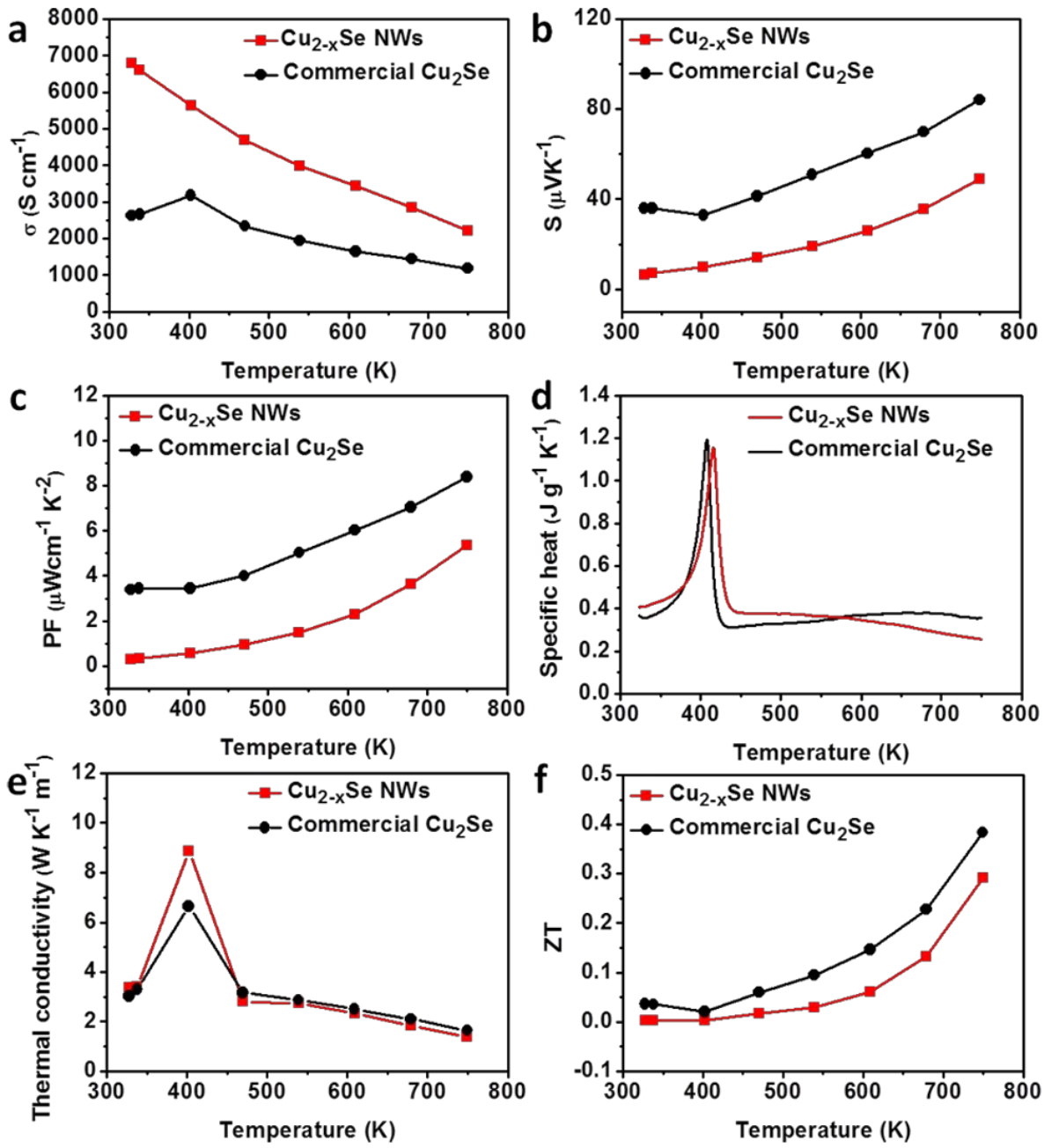

Figure 5. Temperature dependent thermoelectric properties of $Cu_{2-x}Se$ nanowire bundles and commercial Cu_2Se powder: (a) electrical conductivity; (b) Seebeck coefficient; (c) power factor; (d) specific heat (*Cp*); (e) thermal conductivity; and (f) figure-of-merit calculated using Equation (1).

Table 1. Ratio of Cu to Se in the products collected at different reaction time, as determined by ICP-AES.

	1 min	40 min	90 min	3.5 h	5 h	7 h	18 h
Copper (mg/L)	28	23	26	23	26	25	39
Selenium (mg/L)	35	27	24	19	21	20	29
Ratio of Cu to Se	1.01	1.06	1.35	1.51	1.51	1.52	1.65